Photoelectrochemistry

DOI: 10.1002/anie.201206074

# Self-Enhanced Electrochemiluminescence of an Iridium(III) Complex: Mechanistic Insight**

*Kalen N. Swanick, Sébastien Ladouceur, Eli Zysman-Colman,* and Zhifeng Ding**

Heteroleptic cationic iridium complexes have been used as alternative luminophores to neutral *ortho*-metalated iridium complexes (e.g., *fac*-Ir(ppy)$_3$, where ppyH is 2-phenylpyridine) for visual display applications.[1] Single-layer devices known as light-emitting electrochemical cells (LEECs) can now be fabricated, which operate through ion diffusion to opposite electrodes thereby enhancing electronic charge injection at low operating voltages (the so-called electrodynamic model).[2] We have synthesized several cationic iridium complexes of the form [(C^N)$_2$Ir(N^N)], where C^N is a cyclometalating ligand and N^N is a neutral diimine ancillary ligand[3] and explored their optoelectronic properties. We recently have discovered that iridium(III) complexes bearing aryltriazole C^N ligands exhibit bright electrochemiluminescence (or electrogenerated chemiluminescence, ECL), with which ECL efficiency is up to four times greater than that of [Ru(bpy)$_3$]$^{2+}$ upon addition of benzoyl peroxide (BPO) as a co-reactant.[4] Development of such highly efficient and stable ECL emitters over a broad spectrum of wavelengths, as illustrated by the Bard group for other luminophores,[5] has been anticipated for many years, and might find wide applications such as for DNA determination or immunoassay development.[6]

With the goal of obtaining bright true blue-light emitters, we recently investigated the photophysical and ECL properties of ([(dFphtl)$_2$Ir(dmabpy)]$^+$, **1**, [dFphtl = 1-benzyl-4-(2,4-difluoro-phenyl)-1*H*-1,2,3-triazole; dmabpy = 4,4′-(dimethylamino-2,2′-bipyridine); Scheme 1].[7] Though not apparent initially, during subsequent investigation of the ECL behavior of **1**, we realized that we could exploit the redox chemistry of the two dimethylamino (dma) groups on the bpy ligand of **1** and thus enhance its ECL efficiency. This prediction was based on ECL studies using tri-*n*-propylamine (TPrA) as a co-reactant to enhance the ECL and efficiently generate light in organic solvents[8] though TPrA is the most efficient in generating light with luminophores in aqueous media.[6a,9]

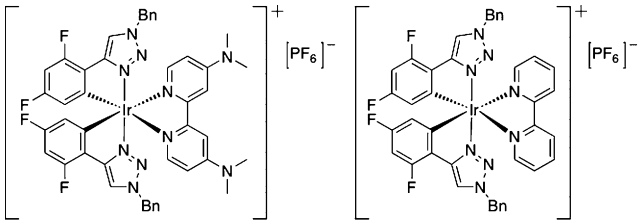


***Scheme 1.*** Iridium(III) complexes [(dFphtl)$_2$Ir(dmabpy)]PF$_6$, **1**, and [(dFphtl)$_2$Ir(bpy)]PF$_6$, **2**.

The classic form of ECL involves electron transfer between electrochemically generated radical ions in solution to produce excited species that emit light.[6a,b] In recent years, the use of TPrA as a co-reactant has been found to be a sensitive technique for biological detections.[6b] Herein, we report the electrochemistry and ECL of **1** in comparison with a structurally similar cationic Ir$^{III}$ complex, [(dFphtl)$_2$Ir(bpy)]$^+$, **2**, (bpy = 2,2′-bipyridine). For the first time, ECL auto-enhancement was observed, with three excited states in the ECL emission of **1** deconvoluted by means of our recently developed ECL spooling technique. By contrast, **2** emitted ECL only at one peak wavelength with no enhancement in the photocurrent. The ECL of **1** was discovered to be self-enhanced with the two dma groups acting as co-reactants. It is conceivable that **1** can be modified with anchoring groups that form bonds with lipids, nucleic acids and proteins for simplified and enhanced ECL detection in biological applications.

Complexes **1** and **2** (Scheme 1), similar in structure to other cationic iridium complexes that we have investigated,[4] show a very good ECL efficiency in acetonitrile (ACN) in the annihilation path when the applied potential was scanned in the range between their first oxidation and first reduction. The pair of cyclic voltammogram (CV) and ECL–voltage curves (in red) of **1** in Figure 1a demonstrated quasi-reversible reduction at −1.82 V [Eq. (1)] and oxidation at 1.42 V [Eq. (2)] versus a saturated calomel electrode (SCE):

$$[(\mathrm{dFphtl})_2\mathrm{Ir}(\mathrm{dma_1bpydma_2})]^+ + e^- \rightarrow [(\mathrm{dFphtl})_2\mathrm{Ir}(\mathrm{dma_1bpydma_2})]^{\bullet} \quad (1)$$

$$[(\mathrm{dFphtl})_2\mathrm{Ir}(\mathrm{dma_1bpydma_2})]^+ \rightarrow [(\mathrm{dFphtl})_2\mathrm{Ir}(\mathrm{dma_1bpydma_2})]^{2+\bullet} + e^- \quad (2)$$

where [(dFphtl)$_2$Ir(dma$_1$bpydma$_2$)]$^+$ represents **1**, with the

[*] K. N. Swanick, Prof. Dr. Z. Ding
Department of Chemistry, The University of Western Ontario
1151 Richmond Street, London, Ontario N6A 5B7 (Canada)
E-mail: zfding@uwo.ca
S. Ladouceur, Prof. Dr. E. Zysman-Colman
Département de Chimie, Université de Sherbrooke
2500 Boulevard de l'Université
Sherbrooke, Quebec J1K 2R1 (Canada)
E-mail: Eli.Zysman-Colman@USherbrooke.ca

[**] This work was supported by NSERC, OCE, PREA, FQRNT, CFI, OIT, UWO, and the Université de Sherbrooke. We thank John Vanstone, Jon Aukema, Yves Rambour, Mary Lou Hart, and Sherrie McPhee for their quality technical support.

Supporting information for this article is available on the WWW under http://dx.doi.org/10.1002/anie.201206079.

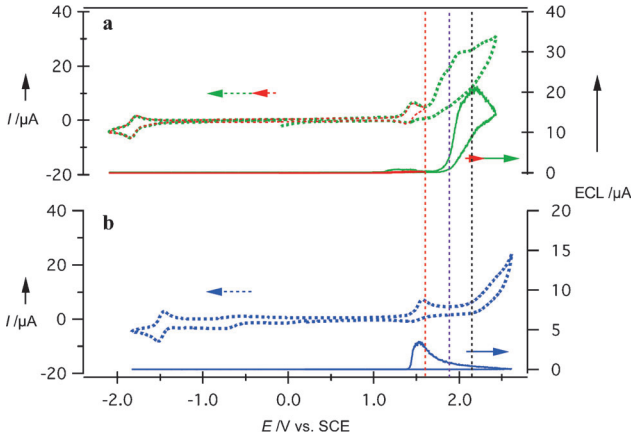


***Figure 1.*** Cyclic voltammograms (dotted) overlaid with corresponding ECL–voltage curves (solid) in acetonitrile of a) 0.6 mM **1** with the applied potential ranges between −2.10 and 1.60 V (in red) and between −2.10 to 2.43 V (in green) vs. a saturated calomel electrode (SCE), and b) of 0.6 mM **2** with the applied potential ranges between −1.80 and 2.60 V (in blue) vs. SCE. The scan rate was at 0.1 $Vs^{-1}$. The vertical dashed lines show the potentials used for estimation of the ECL efficiencies of **1**.

dmabpy ligand now shown as two dma groups attached to bpy.

Complex **1** was found to have an ECL efficiency of 34% (ECL–voltage curve in red, Figure 1a), relative to $[Ru(bpy)_3]^{2+}$.[4,6c,10] Importantly, note that the ECL was only detected after the oxidation reaction, illustrating a higher stability of $[(dFphtl)_2Ir\text{-}(dma_1bpydma_2)]^{\bullet}$ than that of $[(dFphtl)_2Ir(dma_1bpydma_2)]^{2+\bullet}$. While the first reduction reaction was localized on the ancillary ligand,[7] the oxidation originated mainly from Ir as shown by the DFT calculations (see Figure S1 in the Supporting Information).

Upon scanning to higher positive voltages, we found that **1** underwent three further oxidation reactions with peak potentials at 1.75, 1.94, and 2.18 V, respectively (CV in green, Figure 1a). This can be clearly seen from differential pulse voltammograms (DPVs) of **1** (Figure S2 in the Supporting Information). Incredibly, the ECL efficiency in the apparent annihilation process was increased to 550% of that of $[Ru(bpy)_3]^{2+}$ when the positive potential was extended to 2.43 V. Light emission was enhanced 16 times. The ECL efficiency was estimated to be 200 and 400%, respectively, if the applied potential stopped right after the second oxidation (voltage at the vertical purple dashed line, CV curve in green in Figure 1a) or right after the third oxidation reaction (voltage at vertical black dashed line, CV curve in green in Figure 1a). The fourth oxidation reaction appeared not to enhance the ECL efficiency any further though the whole green ECL–voltage curve does give a higher ECL efficiency because of the annihilation reaction continuing in the diffusion layer.

In contrast, **2** did not show the second and third extra oxidation peaks after the similar increases in scan potentials beyond the first oxidation peak (Figure 1b); however, **2** underwent a second oxidation event at a potential shifted 800 mV anodically relative to the first oxidation event, a value similar to the potential difference between the first and fourth oxidation peaks of **1**. Through a comparison of the structures of the two complexes, it is plausible to assign the second and third oxidation waves to iterative oxidation events of the two dma substituents. The fourth oxidation wave probably originated from the oxidation of either the bpy moiety or the C^N ligand. Based on the DFT calculations, it is very likely that this oxidation is localized on the triazole ligand.

The observed ECL enhancement is then due to the presence of the dma substituents on the bpy ligand in **1**, each acting as a self-co-reactant. The mechanisms should be similar to the addition of TPrA to Ru complexes and other luminophores in ECL studies.[6a,8a] Without any self-co-reactant present, the ECL for **2** decayed after the first oxidation (Figure 1b).

Figure 2a shows a magnified section of the ECL spooling spectra of **1** acquired in the first cycle of the potential scanning between −2.10 and 2.42 V. Two cycle scans over 145 s at a scan rate of 0.1 $Vs^{-1}$ were conducted. Each ECL spectrum was acquired for 1 s. Please see Figure S3 in the Supporting Information for the complete spooling spectra for two cycles.

For the first cycle, the scan started at 0.00 V and went to −2.10 V before the scan direction was switched towards positive potential. The ECL spectrum at 1.20 V began to display a weak wave centered at 543 nm, which is close to the photoluminescence (PL) peak wavelength, 495 nm in ACN. The small discrepancy of the ECL and PL wavelengths is probably due to self-absorption given the higher concentra-

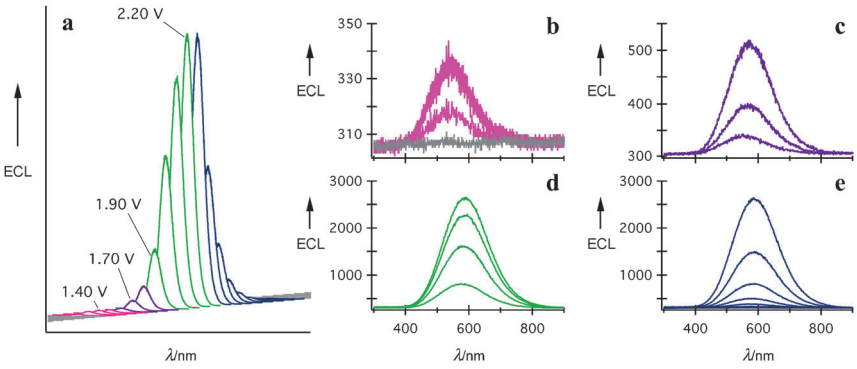


***Figure 2.*** Selected ECL spooling spectra of 0.6 mM **1** in acetonitrile when the applied potential was scanned between −2.10 and 2.42 V for two cycles at a scan rate of 0.1 $Vs^{-1}$, see Figure S3 in the Supporting Information for the two complete cycles. Each ECL spectrum was acquired for 1 s and two scanning cycles took 145 s. a) Perspective view from zoomed-in ECL spooling spectra of the 1st cycle of potential scanning. Three emissions from different excited species are color-coded, with apparent peak positions centered at 543 nm (in pink, b), 566 nm (in purple, c), and 588 nm (in green, d). ECL devolution is illustrated by the spectra in deep blue (e). Three excited states were deconvoluted to peak wavelengths at 543, 608, and 651 nm, respectively, which were generated in annihilation and co-reactant (the two dma groups on the bpy ligand) paths.

tions used in ECL studies.[5e] When the applied potential continued more positive, the ECL wave grew (Figure 2b) and reached a maximum at 1.40 V that is the same as the first maximum potential in the ECL–voltage curve (Figure 1a). ECL evolution (ECL spectra in pink, Figure 2b) in this potential range follows the annihilation mechanism shown in Equations (3) and (4):

$$[(dFphtl)_2Ir(dma_1bpydma_2)]^{\bullet} + [(dFphtl)_2Ir(dma_1bpydma_2)]^{2+\bullet} \rightarrow [(dFphtl)_2Ir(dma_1bpydma_2)]^{+*} + [(dFphtl)_2Ir(dma_1bpydma_2)]^{+} \quad (3)$$

$$[(dFphtl)_2Ir(dma_1bpydma_2)]^{+*} \rightarrow [(dFphtl)_2Ir(dma_1bpydma_2)]^{+} + h\nu_1 \quad (4)$$

In the initial scanning from 0.00 to −2.10 V, $[(dFphtl)_2Ir(dma_1bpydma_2)]^{\bullet}$ radicals were formed upon reduction right after −1.82 V, Equation (1). The applied potential was swept towards positive potentials and $[(dFphtl)_2Ir(dma_1bpydma_2)]^{2+\bullet}$ radical cations were generated with an onset potential of 1.20 V, Equation (2). The two radicals combined in the vicinity of the electrode to yield the excited state species that is responsible for light emission upon relaxation to the ground state [Eqs. (3) and (4)].

Upon further scanning to more positive potentials, the ECL spectrum showed an increase in intensity as depicted in the ECL–voltage curve (green curve in Figure 1a). More importantly, the apparent ECL peak wavelength was red-shifted as illustrated by the purple spectra in Figure 2a, and c. As described above for the cyclic voltammetry, the two dma groups on the bpy ligand can be oxidized consecutively. Immediately after the first oxidation localized on the Ir center, the first dma substituent began to lose one electron to generate $[(dFphtl)_2Ir(dma_1^{+\bullet}bpydma_2)]^{2+\bullet}$, Equation (5). The intermediate might deprotonate once to produce $[(dFphtl)_2Ir(dma_1^{\bullet}bpydma_2)]^{2+\bullet}$, a strong reducing agent [Eq. (6)]. The radical would react with the oxidized complex already present in solution, $[(dFphtl)_2Ir(dma_1bpydma_2)]^{2+\bullet}$, Equation (7), to generate the same excited species as in the annihilation path, $[(dFphtl)_2Ir(dma_1bpydma_2)]^{+*}$, Equation (7). The light emission would follow the same process as described by Equation (4).

$$[(dFphtl)_2Ir(dma_1bpydma_2)]^{2+\bullet} \rightarrow [(dFphtl)_2Ir(dma_1^{+\bullet}bpydma_2)]^{2+\bullet} + e^{-} \quad (5)$$

$$[(dFphtl)_2Ir(dma_1^{+\bullet}bpydma_2)]^{2+\bullet} \rightarrow [(dFphtl)_2Ir(dma_1^{\bullet}bpydma_2)]^{2+\bullet} + H^{+} \quad (6)$$

$$[(dFphtl)_2Ir(dma_1bpydma_2)]^{2+\bullet} + [(dFphtl)_2Ir(dma_1^{\bullet}bpydma_2)]^{2+\bullet} \rightarrow [(dFphtl)_2Ir(dma_1bpydma_2)]^{+*} + [(dFphtl)_2Ir(dma_1^{+}bpydma_2)]^{2+\bullet} \quad (7)$$

There is another pathway where $[(dFphtl)_2Ir(dma_1^{+\bullet}bpydma_2)]^{2+\bullet}$ could react with the radical generated in the cathodic region [Eq. (2)] to yield the second excited species [Eq. (8)]. This excited state could emit light at a different wavelength $h\nu_2$ [Eq. (9)]. Based on this mechanistic proposal, the purple ECL spectra were deconvoluted and fitted to two peaks, the first being fixed at 543 nm and the second being fitted to 608 nm (Figure S4a and S4b in the Supporting Information). The red-shift of the second peak is due to the switch from an electron-donating dma group to an electron-withdrawing $dma^{+\bullet}$ radical on the bpy ligand. As described initially by Nazeeruddin, De Angelis, and Grätzel et al.,[2b,11] the presence of the dma-substitutents on the bipyridine ligand act to significantly destabilize the lowest unoccupied molecular orbitals (LUMO) orbitals, resulting in a large increase in the HOMO–LUMO gap (HOMO = highest occupied molecular orbital). It is conceivable that the electron-withdrawing $dma^{+\bullet}$ would shrink the gap and produce a red-shifted ECL spectrum. Note that the $dma^{+\bullet}$ radical is stabilized by delocalization of the charge throughout the entire bpy ligand.

$$[(dFphtl)_2Ir(dma_1^{+\bullet}bpydma_2)]^{2+\bullet} + [(dFphtl)_2Ir(dma_1bpydma_2)]^{\bullet} \rightarrow [(dFphtl)_2Ir(dma_1^{+\bullet}bpydma_2)]^{+*} + [(dFphtl)_2Ir(dma_1bpydma_2)]^{+} \quad (8)$$

$$[(dFphtl)_2Ir(dma_1^{+\bullet}bpydma_2)]^{+*} \rightarrow [(dFphtl)_2Ir(dma_1^{+\bullet}bpydma_2)]^{+} + h\nu_2 \quad (9)$$

The ECL peak intensity was further enhanced when the scan moved to more positive potentials (green ECL spectra in Figure 2a and d). This trend continued until 2.20 V. In this potential region, the second dma group on the dmabpy ligand can be oxidized, becoming a self-co-reactant like the first dma substituent and generating one additional excited species. The ECL process follows a similar co-reactant mechanism as with $dma_1$ involvement described above. However, now there is the generation of the third excited species, $[(dFphtl)_2Ir(dma_1^{+\bullet}bpydma_2^{+\bullet})]^{1+*}$, emitting at 651 nm, with energy $h\nu_3$ given in Equation (10):

$$[(dFphtl)_2Ir(dma_1^{+\bullet}bpydma_2^{+\bullet})]^{+*} \rightarrow [(dFphtl)_2Ir(dma_1^{+\bullet}bpydma_2^{+\bullet})]^{+} + h\nu_3 \quad (10)$$

The third ECL peak position was obtained in the same manner through a three-component deconvolution of the ECL spectra (green in Figure 2a and d, with the first two curves now fixed at 543 and 608 nm, respectively (Figure S4c in the Supporting Information).

Finally, as the potential continued to increase from 2.21 to 2.42 V then swept back to 0.00 V, a decrease in ECL intensity was observed with the apparent ECL maximum centered at 568 nm until no emission was observed in the ECL (Figure 2e). The flat spectra continued until the ECL progression of the second cycle reached around 1.20 V. The ECL spectra (black in Figure 2a and e) were fitted by curves (Figure S5a–e in the Supporting Information), showing that the three peaks all decreased in intensity as the potential moved first from 2.20 V to 2.42 V and then towards negative potentials.

Over the second cycle, we observed the evolution of the same three ECL peaks as those observed in the first cycle, 543, 608 and 651 nm, indicating a reproducible ECL behavior over subsequent potential scan cycles.

  

In summary, for the first time three different emissions were observed during an ECL process. By means of fitting curves, these three emissions in **1** were deconvoluted from the spooling ECL spectra to be at 543, 608, and 651 nm, correlating to three ECL mechanisms: the first being the typical annihilation route[6b] while the second and third involved a self-co-reactant route implicating the oxidation of dmabpy, similar to the TPrA co-reactant mechanism.[6b,8a] By contrast, **2** only follows the annihilation route because of the absence of dma substituents on the bpy. The ECL efficiency for **1** increased from approximately 35% (annihilation) to 200% (after the second oxidation) to 400% (after the third oxidation) and finally to 550% (after the fourth oxidation). These ECL efficiencies are the highest reported for iridium complexes. Moreover, this dramatic increase in ECL is attributed to the unique architecture of the dmabpy ligand acting as a self-co-reactant in **1**. This may lead to an avenue for greatly simplifying ECL detection protocols with integrated co-reactant and luminophore in a single molecule, and drastically enhancing detection sensitivity up to 16 times.

Received: July 30, 2012
Published online: October 4, 2012

**Keywords:** electrochemiluminescence · electrochemistry · iridium · photoelectrochemistry · quantum efficiencies

[1] a) J. M. Fernández-Hernández, C.-H. Yang, J. I. Beltrán, V. Lemaur, F. Polo, R. Fröhlich, J. Cornil, L. De Cola, *J. Am. Chem. Soc.* **2011**, *133*, 10543 – 10558; b) M. Mauro, K. C. Schuermann, R. Prétôt, A. Hafner, P. Mercandelli, A. Sironi, L. De Cola, *Angew. Chem.* **2010**, *122*, 1244 – 1248; *Angew. Chem. Int. Ed.* **2010**, *49*, 1222 – 1226.

[2] a) J. D. Slinker, A. A. Gorodetsky, M. S. Lowry, J. Wang, S. Parker, R. Rohl, S. Bernhard, G. G. Malliaras, *J. Am. Chem. Soc.* **2004**, *126*, 2763 – 2767; b) F. De Angelis, S. Fantacci, N. Evans, C. Klein, S. M. Zakeeruddin, J.-E. Moser, K. Kalyanasundaram, H. J. Bolink, M. Grätzel, M. K. Nazeeruddin, *Inorg. Chem.* **2007**, *46*, 5989 – 6001; c) R. D. Costa, E. Ortí, H. J. Bolink, S. Graber, S. Schaffner, M. Neuburger, C. E. Housecroft, E. C. Constable, *Adv. Funct. Mater.* **2009**, *19*, 3456 – 3463; d) E. Holder, B. M. W. Langeveld, U. S. Schubert, *Adv. Mater.* **2005**, *17*, 1109 – 1121; e) T. Hu, L. He, L. Duan, Y. Qiu, *J. Mater. Chem.* **2012**, *22*, 4206 – 4215; f) J. D. Slinker, J. Rivnay, J. S. Moskowitz, J. B. Parker, S. Bernhard, H. D. Abruna, G. G. Malliaras, *J. Mater. Chem.* **2007**, *17*, 2976 – 2988; g) R. D. Costa, E. Ortí, H. J. Bolink, F. Monti, G. Accorsi, N. Armaroli, *Angew. Chem.* **2012**, *124*, 8300 – 8334; *Angew. Chem. Int. Ed.* **2012**, *51*, 8178 – 8211.

[3] a) S. Ladouceur, D. Fortin, E. Zysman-Colman, *Inorg. Chem.* **2010**, *49*, 5625 – 5641; b) S. Ladouceur, D. Fortin, E. Zysman-Colman, *Inorg. Chem.* **2011**, *50*, 11514 – 11526.

[4] K. N. Swanick, S. Ladouceur, E. Zysman-Colman, Z. Ding, *Chem. Commun.* **2012**, *48*, 3179 – 3181.

[5] a) A. B. Nepomnyashchii, A. J. Bard, *Acc. Chem. Res.* **2012**, DOI: 10.1021/ar200278b; b) A. B. Nepomnyashchii, R. J. Ono, D. M. Lyons, C. W. Bielawski, J. L. Sessler, A. J. Bard, *Chem. Sci.* **2012**, *3*, 2628; c) J. Suk, K. M. Omer, T. Bura, R. Ziessel, A. J. Bard, *J. Phys. Chem. C* **2011**, *115*, 15361 – 15368; d) K. M. Omer, S.-Y. Ku, K.-T. Wong, A. J. Bard, *Angew. Chem.* **2009**, *121*, 9464 – 9467; *Angew. Chem. Int. Ed.* **2009**, *48*, 9300 – 9303; e) S. Rashidnadimi, T. H. Hung, K.-T. Wong, A. J. Bard, *J. Am. Chem. Soc.* **2008**, *130*, 634 – 639.

[6] a) W. Miao, *Chem. Rev.* **2008**, *108*, 2506 – 2553; b) A. J. Bard, *Electrogenerated Chemiluminescence*, Marcel Dekker, New York, **2004**; c) K. N. Swanick, D. W. Dodd, J. T. Price, A. L. Brazeau, N. D. Jones, R. H. E. Hudson, Z. Ding, *Phys. Chem. Chem. Phys.* **2011**, *13*, 17405 – 17412; d) L. Xu, Y. Li, S. Wu, X. Liu, B. Su, *Angew. Chem.* **2012**, DOI: 10.1002/ange.201203815; *Angew. Chem. Int. Ed.* **2012**, DOI: 10.1002/anie.201203815.

[7] S. Ladouceur, S. Gallagher-Duval, K. N. Swanick, Z. Ding, E. Zysman-Colman, submitted.

[8] a) R. Y. Lai, A. J. Bard, *J. Phys. Chem. A* **2003**, *107*, 3335 – 3340; b) S. K. Lee, M. M. Richter, L. Strekowski, A. J. Bard, *Anal. Chem.* **1997**, *69*, 4126 – 4133; c) W. Miao, A. J. Bard, *Anal. Chem.* **2004**, *76*, 5379 – 5386; d) W. Miao, A. J. Bard, *Anal. Chem.* **2004**, *76*, 7109 – 7113; e) M. M. Richter, A. J. Bard, W. Kim, R. H. Schmehl, *Anal. Chem.* **1998**, *70*, 310 – 318; f) D. J. Vinyard, M. M. Richter, *Anal. Chem.* **2007**, *79*, 6404 – 6409.

[9] a) W. Miao, J.-P. Choi, A. J. Bard, *J. Am. Chem. Soc.* **2002**, *124*, 14478 – 14485; b) F. Kanoufi, Y. Zu, A. J. Bard, *J. Phys. Chem. B* **2001**, *105*, 210 – 216; c) A. W. Knight, G. M. Greenway, *Analyst* **1996**, *121*, 101R – 106R; d) Y. Zu, A. J. Bard, *Anal. Chem.* **2000**, *72*, 3223 – 3232.

[10] a) C. Booker, X. Wang, S. Haroun, J. Zhou, M. Jennings, B. L. Pagenkopf, Z. Ding, *Angew. Chem.* **2008**, *120*, 7845 – 7849; *Angew. Chem. Int. Ed.* **2008**, *47*, 7731 – 7735; b) K. N. Swanick, J. T. Price, N. D. Jones, Z. Ding, *J. Org. Chem.* **2012**, *77*, 5646 – 5655.

[11] M. K. Nazeeruddin, R. T. Wegh, Z. Zhou, C. Klein, Q. Wang, F. De Angelis, S. Fantacci, M. Grätzel, *Inorg. Chem.* **2006**, *45*, 9245 – 9250.

  